

## Template-Dependent Morphogenesis of Oriented Calcite Crystals in the Presence of Magnesium Ions\*\*

Yong-Jin Han, Laura M. Wysocki,  
Monica S. Thanawala, Theo Siegrist, and  
Joanna Aizenberg\*

The ability of biological systems to exert precise control over the shape, size, orientation, and hierarchical ordering of inorganic materials is of great interest to chemists and material scientists.<sup>[1,2]</sup> Potential applications of this biological level of control to the development of new synthetic pathways and to the improvement of existing materials is beginning to be recognized. Biogenic calcium carbonate, one of the most abundant minerals formed by organisms, is a wonderful example of nature's precision. The elaborate and unique morphologies of biogenic calcium carbonates, which in the course of evolution are cleverly refined to accommodate diverse survival functions,<sup>[1-5]</sup> have prompted extensive studies into the mechanism by which they form.<sup>[6,7]</sup> The development of biogenic calcium carbonates was shown to be closely associated with proteins rich in acidic/hydroxy residues<sup>[1,2,4,8]</sup> and with divalent cations, such as magnesium ions.<sup>[9-11]</sup> The formation of crystals with diverse morphologies has been reported by numerous in vitro studies, in which calcite growth was modified by the interaction with various organic and inorganic additives in solution.<sup>[4,12-20]</sup> Although these experiments demonstrated successfully that the morphology of calcite could be altered from its regular {104} cleavage rhombohedron form, the modified crystals were, in general, heterogeneous in their shapes, sizes, and orientations.

In particular, calcite growth in the presence of Mg ions, in both synthetic and sedimentary environments, was shown to result in the formation of elongated crystals that express new pseudofacets that are roughly parallel to the *c*-axis.<sup>[9,13,21-24]</sup> This habit modification was traditionally explained by a face-specific mechanism involving interaction between the Mg ions and calcite surfaces parallel to the *c*-axis<sup>[24]</sup> and recently by a step-specific mechanism involving differential incorporation of Mg ions into nonequivalent steps.<sup>[21]</sup> It has been shown that such interactions between Mg ions and calcite lead to calcite rhombohedra developing characteristic, elongated, roughened seedlike shapes that depend on the ratio of Mg/Ca ions.<sup>[19,21]</sup> The experimental data showed, however, that the sizes of Mg-ion-treated crystals, the extent

of the elongation along the *c*-axis, the ratio between the {104} plane and the new Mg-ion-induced facets, and their precise  $\{hkl\}$  indices were nonuniform, even within the same experiment and under the same conditions. Herein, we report an approach to synthesize arrays of homogeneous calcite crystals in a variety of morphological forms. Crystal growth in the presence of an additive (Mg ions) is coupled with control over the oriented nucleation achieved by using functionalized self-assembled monolayers (SAMs) as nucleation templates.<sup>[25-27]</sup> Experiments performed with a range of template/additive combinations demonstrated the formation of arrays of calcite crystals with highly uniform features (namely, size, shape, orientation, composition, and dynamics of growth), which are characteristic for each surface. We discuss possible mechanisms for this intriguing new phenomenon, which we have termed template-dependent crystal morphogenesis.

The four surfaces used to control the oriented nucleation were Au films functionalized with thiols containing carboxylic acids of odd chain length ( $C_{15}-CO_2H$ ), carboxylic acids of even chain length ( $C_{10}-CO_2H$ ), alcohols ( $C_{11}-OH$ ), and sulfonic acids ( $C_{11}-SO_3H$ ). These species were chosen to correspond to the functional residues of biomolecules commonly associated with biominerals. Although ordered functional groups on surfaces alone do not mimic biomolecules, they do provide insight into the importance of ordered arrays of functional groups that are often displayed on proteins responsible for the regulation of biomineral formation.

Calcite crystals grown on the surfaces of SAMs in the absence of additives were normal {104} rhombohedra that selectively nucleated from different planes induced by the SAM/metal combination.<sup>[26,27]</sup> More than 90% of the crystals grown from the surface functionalized with  $C_{10}-CO_2H$  species nucleated from the (11 $\bar{l}$ ) crystallographic planes of calcite ( $l = 3-4$ ) and more than 95% of crystals templated by the surface functionalized with  $C_{15}-CO_2H$  species nucleated from the (01 $\bar{l}$ ) planes ( $l = 2-5$ ), as shown by X-ray diffraction and morphological analyses (Figure 1 a, b). Interestingly, the surface functionalized with  $C_{11}-SO_3H$  species provided a mixture of crystals with the (106) and (1.0.12) nucleating planes in a ratio of 70:30 (Figure 1 c). This latter observation suggests that the interfacial  $SO_3H$  groups apparently conform to two different orientations/structures upon coordinating with the Ca ions (a possibility that is currently being investigated). More than 98% of the calcite crystals grown on the surfaces functionalized with  $C_{11}-OH$  species selectively nucleated from the (104) plane (Figure 1 d). The size and nucleation densities of the crystals grown on different templates are summarized in Table 1.

Dramatic changes in the crystallization characteristics were observed upon addition of Mg ions to the solution. Small amounts of Mg ions ( $n \leq 0.5$ ,  $n = Mg/Ca$  ions (mol/mol)) induced significant homogenization of crystal sizes for three acid-terminated surfaces with no morphological changes (Table 1). The addition of Mg ions ( $n \leq 0.5$ ) to the crystallizing solution of the SAMs terminated by sulfonic acid groups favored the formation of crystals nucleating from the (106) crystallographic planes and the number of crystals nucleating from the (1.0.12) planes decreased dramatically. This result suggests that Mg ions are involved in the nucleation process,

[\*] Dr. Y.-J. Han, L. M. Wysocki, M. S. Thanawala, Dr. T. Siegrist, Dr. J. Aizenberg  
Bell Laboratories  
Lucent Technologies, 600 Mountain Avenue  
Murray Hill, NJ 07974 (USA)  
Fax: (+1) 908-582-4868  
E-mail: jaizenberg@lucent.com

[\*\*] We thank J. J. DeYoreo, E. DiMasi, and C. Orme for constructive discussions.

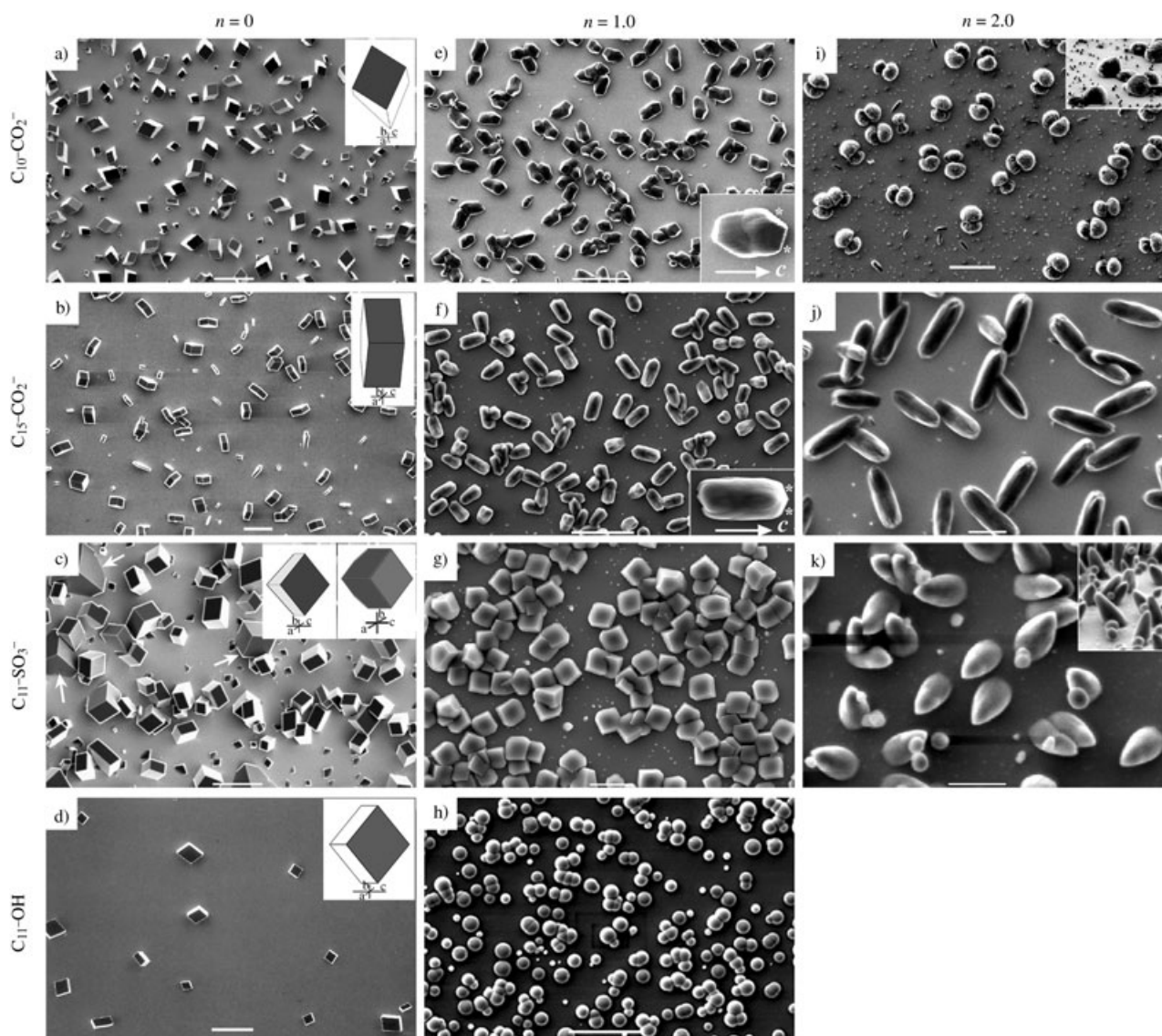


**Figure 1.** SEM images of oriented calcite crystals grown on different organic templates in the presence or absence of Mg ions. The micrographs were recorded on a JEOL JSM-5600 LV system. The SAMs and the ratios of Mg and Ca ions in solution  $n$  are indicated. a)  $C_{10}$ -CO<sub>2</sub>H functionalization,  $n=0$ , scale bar=50  $\mu$ m, inset: computer simulation of the {104} rhombohedron nucleated from the (113) plane. b)  $C_{15}$ -CO<sub>2</sub>H functionalization,  $n=0$ , scale bar=50  $\mu$ m, inset: computer simulation of the {104} rhombohedron nucleated from the ( $\bar{1}$ 03) plane. c)  $C_{11}$ -SO<sub>3</sub>H functionalization,  $n=0$ , scale bar=20  $\mu$ m, insets: computer simulation of the {104} rhombohedron nucleated from the (106) plane (left) and the (1.0.12) plane (right). Crystals in the (1.0.12) orientation are indicated by arrows. d)  $C_{11}$ -OH functionalization,  $n=0$ , scale bar=100  $\mu$ m, inset: computer simulation of the {104} rhombohedron nucleated from the (104) plane. e)  $C_{10}$ -CO<sub>2</sub>H functionalization,  $n=1.0$ , scale bar=50  $\mu$ m, inset: high-magnification SEM analysis showing the morphology of an individual crystal. Although the normal {104} cleavage planes of calcite were still clearly visible (indicated by \*), the crystals develop striated facets roughly parallel to the  $c$ -axis with a narrow center. f)  $C_{15}$ -CO<sub>2</sub>H functionalization,  $n=1.0$ , scale bar=50  $\mu$ m, inset: high-magnification of an individual, morphologically modified cylindrical crystal. g)  $C_{11}$ -SO<sub>3</sub>H functionalization,  $n=1.0$ , scale bar=10  $\mu$ m. Only crystals nucleated from the (106) plane remain. The crystals show no morphological changes. h)  $C_{11}$ -OH functionalization,  $n=1.0$ , scale bar=10  $\mu$ m. Total inhibition of crystallization and the formation of ACC. i)  $C_{10}$ -CO<sub>2</sub>H functionalization,  $n=2.0$ , scale bar=20  $\mu$ m, inset: edge-on view showing the asymmetric orientation of the dumb-bells on the surface. Crystals uniformly develop a dumb-bell shape and ACC spheres start to form. j)  $C_{15}$ -CO<sub>2</sub>H functionalization,  $n=2.0$ , scale bar=10  $\mu$ m. Crystals uniformly develop a cylindrical shape. k)  $C_{11}$ -SO<sub>3</sub>H functionalization,  $n=2.0$ , scale bar=5  $\mu$ m, inset: edge-on view showing that the crystals form a high angle with the surface. Crystals uniformly develop a conical shape.

possibly in two ways: by promoting the preferential alignment of the SO<sub>3</sub>H groups at the SAM interface in the configuration which induces the nucleation of calcite crystals from the (106) plane, and/or by inhibition of the alternative alignment that would favor nucleation from the (1.0.12) plane. Interestingly, total inhibition of crystallization was observed on the surfaces

terminated by  $C_{11}$ -OH species upon the addition of Mg ions ( $n \leq 0.5$ ) and a thin layer of amorphous calcium carbonate (ACC) spheres covered the surface of the SAM. This observation is further evidence that Mg ions do not only act as growth modifiers but are also involved at the nucleation stage as surface reconstruction agents, thus promoting/

**Table 1:** Crystal size, nucleation density, Mg content, and elongation along the *c*-axis for calcite crystals grown on different SAMs in the presence of Mg ions.

SAM	<i>n</i> (Mg/Ca [mol/mol])	Crystal size [μm]		Elongation ratio ( $r=l_c/l_{a,b}$ )	Nucleation density [mm <sup>-2</sup> ]	Mg content in CaCO <sub>3</sub> [mol %]
		along the <i>c</i> -axis ( <i>l<sub>c</sub></i> )	in the <i>a,b</i> plane ( <i>l<sub>a,b</sub></i> )			
C <sub>10</sub> -CO <sub>2</sub> <sup>-</sup>	0:1	23.7 ± 9.2	31.2 ± 8.9	0.7 ± 0.3	1200	0
	0.5:1	19.3 ± 4.1	20.8 ± 3.7	0.9 ± 0.3	1500	6.54
	1.0:1	21.7 ± 2.2	12.1 ± 1.0	1.8 ± 0.2	1600	8.39
	2.0:1	13.1 ± 1.1	5.5 ± 1.0	2.4 ± 0.4	1300	8.8
C <sub>15</sub> -CO <sub>2</sub> <sup>-</sup>	0:1	20.6 ± 8.0	43.8 ± 7.2	0.5 ± 0.2	600	0
	0.5:1	21.7 ± 3.9	19.6 ± 2.1	1.1 ± 0.4	1900	5.96
	1.0:1	25.5 ± 3.6	11.1 ± 0.8	2.3 ± 0.3	3200	9.21
	2.0:1	19.5 ± 2.2	5.8 ± 0.8	3.4 ± 0.6	4400	9.21
C <sub>11</sub> -SO <sub>3</sub> <sup>-</sup>	0:1	6.7 ± 3.9 <sub>(106)</sub>	7.3 ± 4.1 <sub>(106)</sub>	0.9 ± 0.2	10000 <sub>(106)</sub>	0
		15.0 ± 2.1 <sub>(1.0,12)</sub>	14.2 ± 3.2	1.1 ± 0.1	500 <sub>(1.0,12)</sub>	
	0.5:1	5.9 ± 1.9	6.0 ± 1.7	1.0 ± 0.2	25000	5.96
	1.0:1	6.3 ± 0.6	6.4 ± 0.5	1.1 ± 0.1	30000	7.61
	2.0:1	8.3 ± 1.0	2.7 ± 0.3	3.1 ± 0.4	50000	8.99
C <sub>11</sub> -OH	0:1	40.1 ± 10.6	52.0 ± 7.7	0.7 ± 1.2	25	0
	1.0:1		1.7 ± 0.4 <sub>(ACC)</sub>	1	150000	12.8

inhibiting the crystallization process. The formation of the ACC film is consistent with recent studies in which proteins rich in hydroxy residues (namely, serine and threonine) were reported to stabilize ACC in the presence of Mg ions in biological systems.<sup>[10,11,28,29]</sup>

A steady increase in the concentration of Mg ions beyond  $n = 0.5$  further improved the uniformity of the size and shape of the calcite crystals (Table 1). We also observed morphological changes in the regular {104} rhombohedra, in which there were general elongations of the calcite crystals along the *c*-axis (Figure 1e–k). Although the results were highly reproducible and characteristic for each surface type and a given  $n$  value, we detected clear differences in the morphogenesis of calcite crystals grown on the SAMs terminated by C<sub>10</sub>-CO<sub>2</sub>H, C<sub>15</sub>-CO<sub>2</sub>H, and C<sub>11</sub>-SO<sub>3</sub>H species, with the final modified morphologies and crystal shapes being distinctive for each surface type. In particular, progressive asymmetric development and morphological modification of calcites that had been treated with Mg ions yielded arrays of uniform “dumb-bell”-shaped crystals<sup>[30,31]</sup> on the surfaces terminated by the C<sub>10</sub>-CO<sub>2</sub>H species (Figure 1e,i), tapered cylinder-shaped crystals on the surfaces terminated by the C<sub>15</sub>-CO<sub>2</sub>H species (Figure 1f,j), and conical-shaped crystals on the surfaces terminated by the C<sub>11</sub>-SO<sub>3</sub>H species (Figure 1g,k).

Moreover, each surface type exhibited differences in the following parameters of the morphogenesis: 1) the ratio  $n_0$  of Mg and Ca ions in the crystallizing solution at which the appearance of the new faces was detected; 2) the extent of the elongation along the *c*-axis ( $r=l_c/l_{ab}$ ) and the ratio between the {104} plane and new faces induced by Mg ions for a given  $n$  value; 3) the ratio  $n_{Mg}$  of Mg and Ca ions at which the {104} habit disappears and the crystals exhibit only new facets induced by Mg ions, 4) the ratio  $n_{Mg,ACC}$  of Mg and Ca ions at which the ACC phase starts to form and coexists with the calcite crystals; 5) the ratio  $n_{ACC}$  of Mg and Ca ions at which total inhibition of crystallization and the formation of ACC

occurs. These parameters are summarized schematically in Figure 2.

We observed a gradual increase in the incorporation of Mg ions into the calcite crystals as the amount of Mg ions in the crystallizing solution increased (Table 1). This incorporation followed a near-linear trend in the crystalline material and, generally, increased abruptly in the ACC phase.

Our results show unequivocally that the same growth modifier imposes different morphological changes on crystals nucleated from different organic templates even at the same supersaturation levels and impurity concentrations. Two mechanisms may account for this new observation: 1) The desorption of organic molecules from the SAMs would result in their cooperative interaction with the Mg ions and the growing crystals. Each surface would then produce a specific additive combination that may have a distinct effect on crystal morphogenesis. 2) The interaction between

the crystal and the additive, and therefore the resulting morphology, may depend on the orientation of the crystal on the surface.

The first hypothesis was verified by control experiments to test in which trace amounts of one thiol were added together with Mg ions ( $n = 2.0$ ) to a reaction vessel that contained a substrate functionalized with the SAM of a different thiol. Such an addition should change the morphology of the

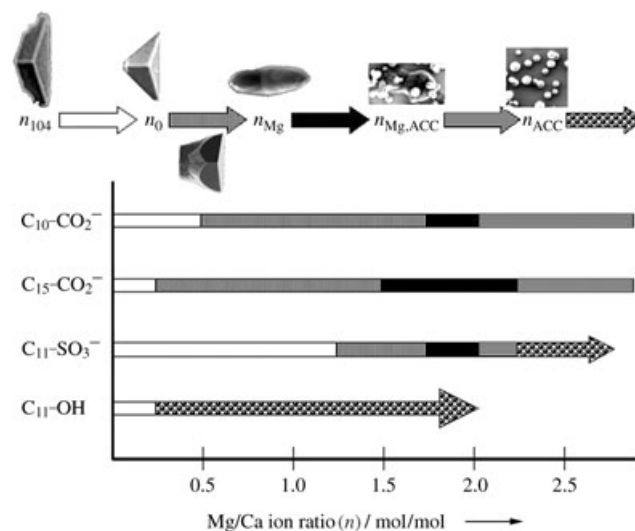


**Figure 2.** Schematic representation that shows the morphogenetic stages of calcite crystals as a function of  $n$  values for different SAMs. The range of  $n$  values from  $n_{104}$  to  $n_0$  indicates the stage at which no morphological changes in calcite crystals were detected. The range from  $n_0$  to  $n_{Mg}$  indicates the stage for which both {104} and the new Mg-modified faces coexist. The range from  $n_{Mg}$  to  $n_{Mg,ACC}$  indicates the stage for which only fully developed Mg-affected crystals form. The range from  $n_{Mg,ACC}$  to  $n_{ACC}$  indicates the stage in which the ACC phase coexists with the treated crystals. Only the ACC phase is observed after  $n_{ACC}$ .

resulting crystals if the first mechanism was correct; for example, the pointed conical shape should change to the dumb-bell shape on addition of the HS-(CH<sub>2</sub>)<sub>10</sub>-CO<sub>2</sub>H thiol to the solution if a SAM of the HS-(CH<sub>2</sub>)<sub>11</sub>-SO<sub>3</sub>H thiol is used as a template. However, no apparent changes in the resulting morphologies were observed.

The second hypothesis was verified by two different experiments: First, we precipitated calcium carbonate in the presence of Mg ions ( $n = 1.25$ ) on a methyl-terminated SAM (a monolayer that does not induce the oriented nucleation and produces an array of randomly oriented calcite crystals).<sup>[27]</sup> The concentration of Mg ions was chosen to correspond to the interval that resulted in the most pronounced differences in crystal morphogenesis (see Figure 2). We observed that the extent of the morphological modification differed significantly between differently oriented crystals, although the same organic molecule may have leaked into their vicinity. We also noticed that the crystal shapes had a tendency to change from conical to cylindrical as the orientation of their *c*-axes changed from being perpendicular to being parallel to the substrate. This observation is consistent with the different shapes of the crystals that had been grown on the surface terminated with sulfonic acid groups and the surface terminated with carboxylic acid groups, where the angle between the *c*-axis and the SAM is approximately 57 and 23°, respectively (Figure 1 j,k). In the second experiment, calcite crystals were grown epitaxially on a biogenic calcite crystal<sup>[13,32]</sup> (echinoderm skeletal elements) in the presence of Mg ions. The surfaces of the echinoderm crystals are round and, therefore, are oriented differently at different locations with respect to the *c*-axis of the constituent calcite. In this experiment, the combined morphological effect of the Mg ions and macromolecules bleaching from the biogenic substrate was studied. Indeed, different morphologies were observed for differently oriented crystals: crystals nucleated at surfaces that were roughly perpendicular to the *c*-axis were conical, while crystals nucleated at surfaces that were parallel to the *c*-axis were cylindrical (Figure 3).

These control experiments confirm that morphological changes induced by a growth modifier depend primarily on the orientation of the crystal on the surface. For randomly oriented crystals, differences in the relative orientation of the crystal surfaces or steps that are specifically recognized by an additive will cause variations in the availability/reactivity of these sites for interaction as well as the difference in the diffusion of an additive toward these sites and, therefore, variations in the concentration of an additive necessary to promote morphological change. These possible variations would lead ultimately to distinct orientation-dependent morphological changes. The same mechanism can be applied successfully to explain the observed uniformity of similarly oriented crystals. In the latter case, the availability of the interacting planes to the additive and, thus, the modification of crystal growth is identical for all crystals, and so homogeneous, characteristic changes in crystal size and morphology will result.

Although we do not exclude the possible, additional effect of the desorbed organic molecules, we believe that they play a secondary role in the observed shape changes when present in

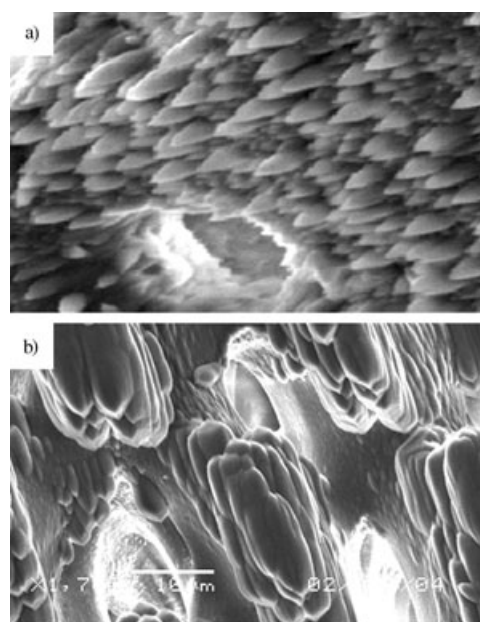


**Figure 3.** Epitaxial overgrowth of synthetic calcite crystals on the surface of biogenic calcite (lateral arm plate of a brittle star) in the presence of Mg ions. Note that a) the crystals grown on surfaces roughly perpendicular to the *c*-axis have a highly tapered, conical shape, while b) the crystals grown on surfaces roughly parallel to the *c*-axis have a cylindrical shape.

low concentrations (such as in the case of SAMs). Our results suggest that the effect of the organic substrate, as well as inducing the orientated nucleation, may include sequestering of Mg ions from the solution. The extent of complexation depends on the chemistry of the organic substrate<sup>[33]</sup> and would be manifested in the differences in the threshold values  $n_0$  required for morphological changes to occur, as was indeed demonstrated in our experiments (Figure 2).

In conclusion, we have described the new phenomenon of template-dependent crystal morphogenesis. We have shown that the effect of a solution growth modifier on crystal shape and size depends on the orientation of the crystals on the surface. The resulting crystal arrays grown from a specific organic template that induces oriented nucleation of the crystals from the same plane are highly uniform in size, morphology, and orientation, which is characteristic of the template/additive combination. We have also presented interesting evidence that Mg ions are involved in the nucleation process and that surfaces functionalized with hydroxy groups can stabilize the formation of amorphous calcium carbonates with few Mg ions present. The impressive crystal homogeneity that is achieved when the addition of a specific crystal growth modifier is coupled with oriented nucleation suggests that the above approach can be used as a powerful synthetic route to crystalline materials with finely tailored morphologies.

### Experimental Section

SAMs were prepared by soaking a 50-nm gold film, which had been prepared by evaporation with an E-beam onto a Si(100) wafer primed

with a 2-nm Ti layer, in 5 mM solutions of HS-(CH<sub>2</sub>)<sub>11</sub>-OH, HS-(CH<sub>2</sub>)<sub>10</sub>-CO<sub>2</sub>H, HS-(CH<sub>2</sub>)<sub>15</sub>-CO<sub>2</sub>H, or HS-(CH<sub>2</sub>)<sub>11</sub>-SO<sub>3</sub>H in alcohol for a minimum of 6 h.<sup>[27]</sup> Calcium carbonate was precipitated on the SAMs by using stock solutions of CaCl<sub>2</sub> (25 mM), MgCl<sub>2</sub> (25 mM, 150 mM), and (NH<sub>4</sub>)HCO<sub>3(s)</sub>, as described in our previous reports.<sup>[25–27]</sup> Experiments were carried out in a cell-culture multidish containing 24 reaction vessels. Every reaction vessel was filled with 2 mL of CaCl<sub>2</sub> (25 mM stock solution) with an appropriate amount of MgCl<sub>2</sub> (25 or 150 mM stock solution) and H<sub>2</sub>O to give a total volume of 4 mL.

The magnesium to calcium ratios  $n$  ( $n = \text{Mg}/\text{Ca}$  ions (mol/mol)) were varied from 0 to 4 with increments of 0.25. Crystallization was carried out simultaneously for all the SAMs and at six different values of  $n$  in the same culture dish to ensure identical experimental conditions for a reliable comparison between different substrates and various  $n$  values. The substrates were always completely submerged beneath the solution/air interface for consistency in crystallization. The crystallization took place inside a desiccator at room temperature over 2 h. Each substrate was then rinsed with H<sub>2</sub>O and dried with compressed nitrogen gas. The crystals were characterized by scanning electron microscopy (SEM) with energy dispersion X-ray attachment (EDX), X-ray diffraction (XRD) using Cu<sub>K $\alpha$</sub>  radiation, and computer simulation of the morphology by using a SHAPE 6.0 program. The Mg content in the precipitate was measured using EDX over a large area that represented a statistical number of crystals and/or ACC particles.

Received: October 13, 2004

Published online: February 28, 2005

**Keywords:** crystal growth · magnesium calcite · morphogenesis · template synthesis

- [1] H. A. Lowenstam, S. Weiner, *On Biomineralization*, Oxford University Press, Oxford, **1989**.
- [2] S. Mann, *Biomineralization: Principles and Concepts in Bioinorganic Materials Chemistry*, Oxford University Press, Oxford, **2001**.
- [3] J. Aizenberg, A. Tkachenko, S. Weiner, L. Addadi, G. Hendler, *Nature* **2001**, *412*, 819.
- [4] L. Addadi, S. Weiner, *Proc. Natl. Acad. Sci. USA* **1985**, *82*, 4110.
- [5] S. A. Wainwright, W. D. Biggs, J. D. Currey, J. M. Gosline, *Mechanical Design in Organisms*, Wiley, New York, **1976**.
- [6] F. C. Meldrum, *Int. Mater. Rev.* **2003**, *48*, 187.
- [7] K. J. Davis, P. M. Dove, J. J. De Yoreo, *Science* **2000**, *290*, 1134.
- [8] G. Falini, S. Albeck, S. Weiner, L. Addadi, *Science* **1996**, *271*, 67.
- [9] S. Raz, S. Weiner, L. Addadi, *Adv. Mater.* **2000**, *12*, 38.
- [10] S. Raz, P. C. Hamilton, F. H. Wilt, S. Weiner, L. Addadi, *Adv. Funct. Mater.* **2003**, *13*, 480.
- [11] J. Aizenberg, G. Lambert, S. Weiner, L. Addadi, *J. Am. Chem. Soc.* **2002**, *124*, 32.
- [12] J. Aizenberg, J. Hanson, T. F. Koetzle, S. Weiner, L. Addadi, *J. Am. Chem. Soc.* **1997**, *119*, 881.
- [13] S. Albeck, J. Aizenberg, L. Addadi, S. Weiner, *J. Am. Chem. Soc.* **1993**, *115*, 11 691.
- [14] C. A. Orme, A. Noy, A. Wierzbicki, M. T. McBride, M. Grantham, H. H. Teng, P. M. Dove, J. J. DeYoreo, *Nature* **2001**, *411*, 775.
- [15] D. B. DeOliveira, R. A. Laursen, *J. Am. Chem. Soc.* **1997**, *119*, 10627.
- [16] J. Donners, R. J. M. Nolte, N. Sommerdijk, *J. Am. Chem. Soc.* **2002**, *124*, 9700.
- [17] M. J. Olszta, S. Gajjaraman, M. Kaufman, L. B. Gower, *Chem. Mater.* **2004**, *16*, 2355.
- [18] H. Colfen, M. Antonietti, *Langmuir* **1998**, *14*, 582.
- [19] J. J. De Yoreo, P. M. Dove, *Science* **2004**, *306*, 1301.
- [20] S. H. Yu, H. Colfen, M. Antonietti, *J. Phys. Chem. B* **2003**, *107*, 7396.
- [21] K. J. Davis, P. M. Dove, L. E. Wasylenki, J. J. De Yoreo, *Am. Mineral.* **2004**, *89*, 714.
- [22] F. Lippmann, *Sedimentary Carbonate Minerals*, Springer, New York, **1973**.
- [23] J. Paquette, R. J. Reeder, *Geology* **1990**, *18*, 1244.
- [24] R. L. Folk, *J. Sediment. Petrol.* **1974**, *44*, 40.
- [25] Y. J. Han, J. Aizenberg, *J. Am. Chem. Soc.* **2003**, *125*, 4032.
- [26] Y. J. Han, J. Aizenberg, *Angew. Chem.* **2003**, *115*, 3796; *Angew. Chem. Int. Ed.* **2003**, *42*, 3668.
- [27] J. Aizenberg, A. J. Black, G. H. Whitesides, *J. Am. Chem. Soc.* **1999**, *121*, 4500.
- [28] L. Addadi, S. Raz, S. Weiner, *Adv. Mater.* **2003**, *15*, 959.
- [29] J. Aizenberg, G. Lambert, L. Addadi, S. Weiner, *Adv. Mater.* **1996**, *8*, 222.
- [30] H. Colfen, L. M. Qi, *Chem. Eur. J.* **2001**, *7*, 106.
- [31] D. Kralj, J. Kontrec, L. Brecevic, G. Falini, V. Nothig-Laslo, *Chem. Eur. J.* **2004**, *10*, 1647.
- [32] J. Aizenberg, S. Albeck, S. Weiner, L. Addadi, *J. Cryst. Growth* **1994**, *142*, 156.
- [33] The relative distribution of Ca and Mg ions between the organic surface and the crystallization solution for different SAMs will be reported elsewhere.